Selected papers presented at the 14th Symposium of Magnetic Measurements and Modelling SMMM'2023

Comparison of Rayleigh Model and Steinmetz Law in Evaluation of Hysteresis Losses in Low Magnetizing Fields

M. Kachniarz*

Warsaw University of Technology, Institute of Metrology and Biomedical Engineering, A. Boboli 8, 02-525 Warszawa, Poland

Doi: 10.12693/APhysPolA.146.64 *e-mail: maciej.kachniarz@pw.edu.pl

The purpose of the following paper is to compare the applicability of Rayleigh hysteresis model and Steinmetz law in the evaluation of power losses of selected soft magnetic materials under the influence of low magnetizing fields. Both approximations are relatively simple in terms of computational complexity, thus they seem to be appropriate for technical applications that do not require extensive knowledge of the physical properties of the material. The selected soft magnetic materials, i.e., steels and ferrites, in the form of toroidal cores, were investigated in low magnetizing fields with a computer-controlled hysteresisgraph system. Both considered models were applied to the obtained power loss characteristics. The quality of the description provided by each model was compared in terms of root-mean-square deviation and determination coefficient R^2, which allowed us to choose the more suitable approximation.

topics: root-mean-square deviation, power loss, Rayleigh model, Steinmetz law

1. Introduction

Measurement and evaluation of power losses of inductive components seem to be crucial in terms of energy saving and reducing CO_2 emission in modern industry. About 285 TWh is lost annually in distribution transformers of power grids only [1], not taking into account losses of inductive components massively widespread in electronic devices.

Modeling of power losses in medium and high magnetizing fields is relatively complex. It can be performed utilizing elaborated physical models of magnetic hysteresis, like the Preisach model or the Jiles–Atherton model [2], by numerical integration of the computed hysteresis loop. However, it seems ineffective in engineering practice where simplicity of calculation is an important factor. Also, physical models dedicated to hysteresis losses, like the Pry and Bean model [3–5] or the Bertotti model [6–9], are not easily applicable, as they require knowledge of multiple microstructural parameters of the material. Moreover, these models are based either on special functions, like the modified Bessel function of the first kind in the Pry and Bean model, or on the time derivative of the magnetic flux density, which is computable only for basic waveform shapes (sinusoidal, triangular). For technical applications, models based on elementary functions and not necessarily involving microstructural parameters seem to be more suitable. Fortunately, in the case of low magnetizing fields of the so-called Rayleigh region, there is a possibility of utilizing such a model, as power losses can be approximated with the Rayleigh hysteresis model or Steinmetz law. Both are relatively simple mathematical approximations, based on second-order polynomial and power function, respectively, so they meet the established requirement of low computational complexity.

In the paper, the effectiveness of both approximations is compared on the set of measurement data including low-field power losses of four soft magnetic materials, i.e., two Ni–Zn ferrites and two structural steels. The quality of the approximation is expressed by means of normalized root-mean-square deviation (NRMSD) between the model and measurement data and determination coefficient R^2.

2. Investigated power loss models

The subject of investigation are two power loss models applicable for low magnetizing field regions. Both are simple mathematical approximations, convenient for technical applications.

The low magnetizing field region (Rayleigh region) is an initial part of the magnetization curve, where the macroscopic magnetization process is mostly governed by elastic deflections and translations of the domain walls, which give rise to the reversible and irreversible components of magnetization, respectively [10]. Therefore, magnetic hysteresis occurs in this region, however, the hysteresis loop exhibits a peculiar shape, sometimes referred to as a lenticular loop [11, 12] or Rayleigh loop [13, 14]. The shape results from both branches of the loop being symmetrical second-order curves, whose intersection points are vertices of the loop. The commutation curve, composed of these vertices, follows the second-order equation known as Rayleigh law of magnetization [10, 13–15], i.e.,

$$B(H) = \mu_0 \left(\mu_i H + \nu_R H^2\right), \quad (1)$$

where B is magnetic flux density, H — magnetizing field, μ_i — initial relative magnetic permeability, ν_R — so-called Rayleigh coefficient, and $\mu_0 = 4\pi \times 10^{-7}$ H/m — magnetic permeability of free space. The linear term refers to a reversible component of magnetization, while the quadratic term describes an irreversible component giving rise to the magnetic hysteresis.

The Rayleigh hysteresis model was first introduced by Lord Rayleigh in 1887 [16]. The basis of the model is the assumption of linear dependence of relative magnetic permeability μ on the magnetizing field H [10, 13]

$$\mu(H) = \mu_i + \nu_R H, \quad (2)$$

which underlies the law of magnetization (1). Moreover, Rayleigh came to the realization that the lenticular hysteresis loop observed in the weak magnetizing field could be also described with the second-order equation, which for descending (upper) branch takes the form [10, 13, 14]

$$B_{\searrow}(H) = \mu_0 \left[\left(\mu_i + \nu_R H_m\right) H + \frac{\nu_R}{2}\left(H_m^2 - H^2\right)\right], \quad (3)$$

and for ascending (lower) branch

$$B_{\nearrow}(H) = \mu_0 \left[\left(\mu_i + \nu_R H_m\right) H - \frac{\nu_R}{2}\left(H_m^2 - H^2\right)\right], \quad (4)$$

where H_m is the amplitude of the magnetizing field. Later, on the basis of (3) and (4), equations describing specific parameters of the hysteresis loop were formulated, including coercive field, magnetic remanence, and energy loss density in the magnetization cycle. Due to the hysteresis loop being described by continuous functions that can be integrated, it is possible to provide an analytical formula for power loss. Total energy loss density corresponds to the surface area of the hysteresis loop [7, 10]

$$w_H = \int_{-B_m}^{B_m} \mathrm{d}B \; H(B), \quad (5)$$

with B_m being the maximum value of magnetic flux density. Note that (5) originates from the calculation of loop area A_H, so geometrically it is a product of the double integral over the surface limited by the $B_{\searrow}(H)$ and $B_{\nearrow}(H)$ functions. The form of total energy loss given by (5), most often provided in the literature, is obtained by changing the order of integration. However, in the Rayleigh region, the straight dependence between magnetic flux density and magnetizing field is known, as $B_{\searrow}(H)$ and $B_{\nearrow}(H)$ are given by (3) and (4), respectively. Therefore, the natural order of integration is more suitable. As the domain of integration can be considered as area A_H limited by magnetizing field extrema H_m and $-H_m$ and branches of the hysteresis loop $B_{\searrow}(H)$ and $B_{\nearrow}(H)$, (5) can be expressed by means of the double integral over the area A_H enclosed by hysteresis loop

$$w_H = \iint_{A_H} \mathrm{d}H \, \mathrm{d}B = \int_{-H_m}^{H_m} \mathrm{d}H \int_{B_{\nearrow}(H)}^{B_{\searrow}(H)} \mathrm{d}B = \int_{-H_m}^{H_m} \mathrm{d}H \left(B_{\searrow}(H) - B_{\nearrow}(H)\right). \quad (6)$$

After substitution, one can obtain

$$w_H = \int_{-H_m}^{H_m} \mathrm{d}H \; \mu_0 \Big(\mu_i H + \nu_R H_m H + \frac{\nu_R}{2} H_m^2 - \frac{\nu_R}{2} H^2 - \mu_i H - \nu_R H_m H + \frac{\nu_R}{2} H_m^2 - \frac{\nu_R}{2} H^2\Big), \quad (7)$$

which leads to

$$w_H = \mu_0 \alpha_R \int_{-H_m}^{H_m} \mathrm{d}H \; \left(H_m^2 - H^2\right) = \mu_0 \nu_R \left(H_m^2 \, 2H_m - \frac{2H_m^3}{3}\right) = \mu_0 \nu_R \left(2H_m^3 - \frac{2}{3} H_m^3\right). \quad (8)$$

This finally results in the expression of dependence between energy loss density w_H and magnetizing field amplitude H_m in the Rayleigh region [7, 13]

$$w_H\left(H_m\right) = \frac{4}{3}\, \mu_0 \nu_R \, H_m^3. \quad (9)$$

Therefore, the expression for power loss during dynamic magnetization in a low magnetizing field region takes the form

$$P_H\left(H_m\right) = f V_e \, \frac{4}{3}\, \mu_0 \nu_R \, H_m^3, \quad (10)$$

where f is the magnetizing field frequency, and V_e — effective volume of the magnetic material.

The Steinmetz law, in its basic form, was originally introduced in 1890 [17]. The dependence of the energy loss density on the maximum magnetic flux density takes the form of a simple power function [17, 18]

$$w_H(B_m) = \alpha B_m^{\eta}. \quad (11)$$

Exponent η is called the Steinmetz exponent (originally reported to be 1.6 [17]), and α is a proportionality factor. Thus, the power loss can be expressed as

$$P_H(B_m) = f V_e \alpha B_m^{\eta}. \quad (12)$$

TABLE I

Main magnetic properties of the investigated soft magnetic materials: $Ni_{0.36}Zn_{0.64}Fe_2O_4$ (A), $Ni_{0.36}Zn_{0.67}Fe_{1.97}O_4$ (B), X30Cr13 (C), and 13CrMo4-5 (D).

Material	A	B	C	D
B_m [T]	0.325	0.260	1.280	1.590
H_c [A/m]	45	95	785	670
B_r [T]	0.120	0.087	0.940	1.245
μ_i [−]	600	250	100	80
V_e [cm^3]	21.04	22.44	2.52	2.52

On the basis of the original Steinmetz law, numerous modifications were developed to better adapt it to the nonlinear character of the magnetization process [19]. A further extension of the power-function-based approximation are models based on the Widom scaling procedure [20, 21]. However, in the case of a low magnetizing field, the magnetic flux density waveform is relatively less distorted from the shape of the magnetizing waveform. Therefore, the nonlinearity of the magnetization process is less meaningful, and expression (12), based on the original Steinmetz equation, might be utilized for power loss approximation.

3. Investigated materials and measurement methodology

Four soft magnetic materials were selected for the experiment. Two of them were ferromagnetic ceramic materials (ferrites) of chemical composition $Ni_{0.36}Zn_{0.64}Fe_2O_4$ and $Ni_{0.36}Zn_{0.67}Fe_{1.97}O_4$, utilized for magnetic cores of wideband transformers and inductive coils. The other two were structural alloy steels X30Cr13 and 13CrMo4-5, used in the power industry. The main magnetic properties of the materials are summarized in Table I. In the case of ferrites, the presented data are provided according to the specification of the manufacturer — POLFER S.A. Maximum magnetic flux density B_m, coercive field H_c, and magnetic remanence B_r provided for steels were previously measured in the saturation region (H_m = 5 kA/m). Initial magnetic permeability μ_i of steels was previously determined for the frame-shaped samples used in magnetoelastic investigation [22, 23].

Investigated materials were formed into toroidal cores, providing a closed magnetic circuit within the sample in order to reduce the demagnetizing field [7]. Each sample was characterized by the effective volume V_e, calculated on the basis of geometrical dimensions of the sample.

The measurements were performed with a digitally controlled hysteresisgraph system. Dynamic magnetic characteristics of all four materials were investigated with the linearly changing magnetizing field (triangle waveform). The magnetizing field frequency for ferrites was 1.0 Hz, while for steels, it was 0.1 Hz. Such low frequencies allowed to significantly reduce the eddy current losses [24], especially in the case of steels. Thus, equation (5), in this case, describes the pure magnetic hysteresis losses.

For each material, a family of several hysteresis loops was measured with increasing values of the magnetizing field amplitude H_m. The limits of H_m corresponding to the Rayleigh region for investigated materials were established according to the values previously presented in paper [25]. Among other parameters, measured loops were characterized by the power loss P_H, which allowed us to obtain the characteristics of P_H as a function of maximum magnetic flux density B_m. All measurements were performed in standard laboratory conditions.

4. Results and discussion

On the basis of experimental results, the characteristics of power loss P_H were determined for the investigated materials. In order to provide a clear reference for both models, the dependence of P_H on maximum magnetic flux density B_m is presented.

The Rayleigh model coefficients of investigated materials were already determined in the previous research [25]. As can be seen in (12), only the Rayleigh coefficient ν_R affects the modeled value of power loss P_H. Coefficients of the Steinmetz law (10) were determined by means of linear regression. Applying natural logarithm to both sides of (12) leads to the expression

$$\ln(P_H) = \ln(fV_e\alpha) + \eta\ln(B_m), \quad (13)$$

thus reducing the problem to linear dependence $y = b + ax$. Linear regression provides directly the value of $\eta = a$, while α is given as

$$\alpha = \frac{e^b}{fV_e}. \quad (14)$$

The determined values of coefficients are presented in Table II. The values of Steinmetz exponent η significantly exceed the original value of 1.6. However, it has to be noted that the presented results were obtained with a non-sinusoidal magnetic flux density waveform. This may lead to the increased exponent η, as well as to a more rapid failure of the model in approximation of power losses with B_m increasing further outside the Rayleigh region, where the nonlinearity of the magnetization process is getting more significant.

Model curves calculated with designated coefficients were applied to the experimental results and are presented in Figs. 1–4. The lower values of power loss for steels result from a much lower effective volume V_e of the steel cores used in the experiment (Table I).

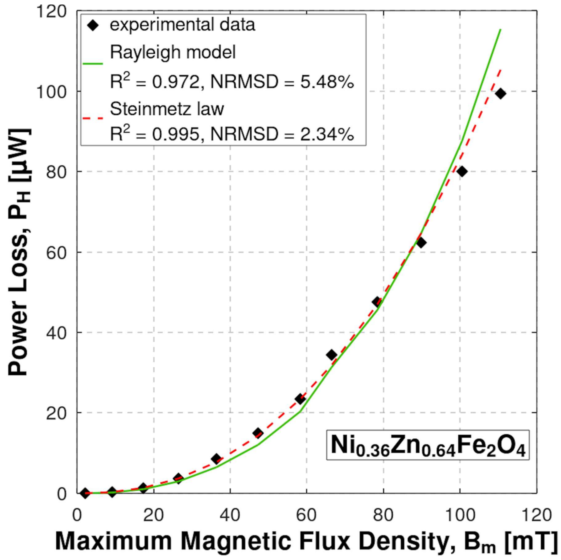

Fig. 1. Results of measurement and modeling of power loss P_H with Rayleigh model and Steinmetz law for $Ni_{0.36}Zn_{0.64}Fe_2O_4$ ferrite.

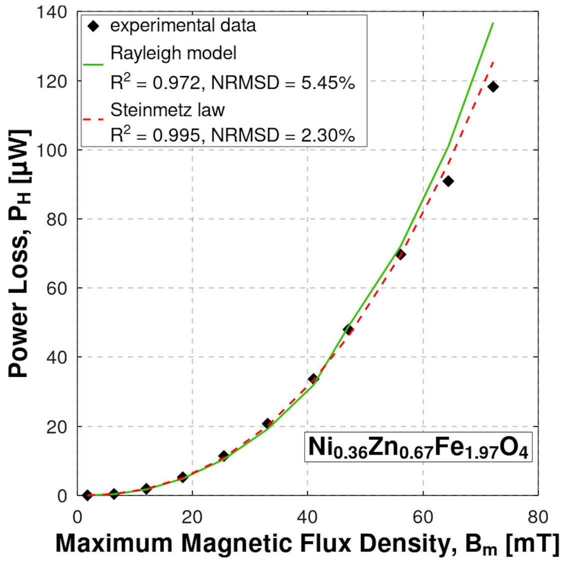

Fig. 2. Results of measurement and modeling of power loss P_H with Rayleigh model and Steinmetz law for $Ni_{0.36}Zn_{0.67}Fe_{1.97}O_4$ ferrite.

TABLE II

Determined values of coefficients of Rayleigh model [25] and Steinmetz law for investigated materials: $Ni_{0.36}Zn_{0.64}Fe_2O_4$ (A), $Ni_{0.36}Zn_{0.67}Fe_{1.97}O_4$ (B), X30Cr13 (C), and 13CrMo4-5 (D).

Material	Rayleigh model		Steinmetz law	
	μ_i [–]	ν_R [m/A]	α [–]	η [–]
A	644	10.45	881.63	2.35
B	285	1.90	2634.63	2.34
C	69	0.16	23456.43	2.69
D	64	0.79	5336.49	2.41

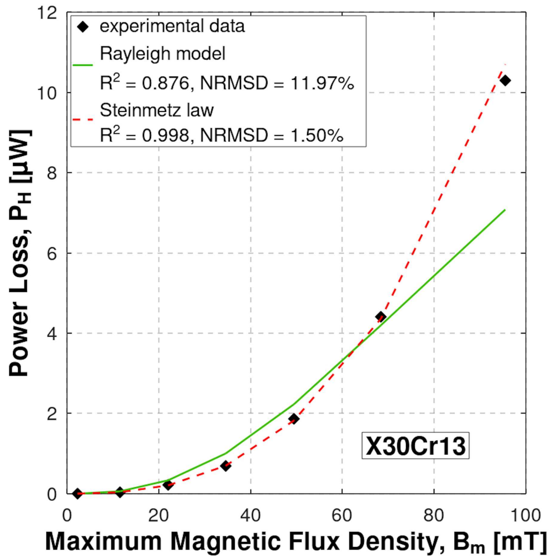

Fig. 3. Results of measurement and modeling of power loss P_H with Rayleigh model and Steinmetz law for X30Cr13 steel.

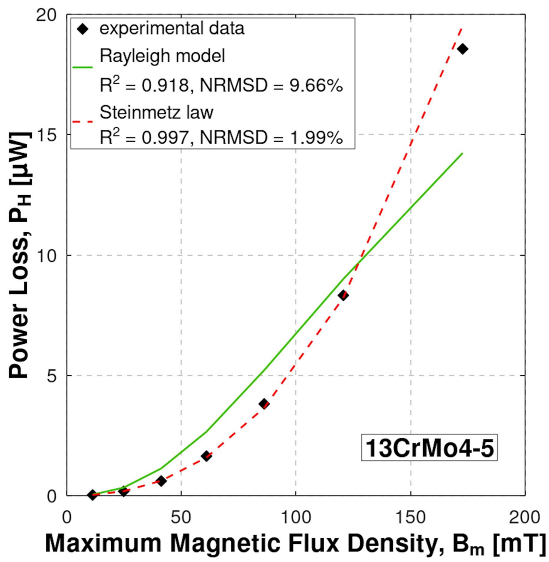

Fig. 4. Results of measurement and modeling of power loss P_H with Rayleigh model and Steinmetz law for 13CrMo4-5 steel.

In the case of Ni–Zn ferrites (Figs. 1 and 2), both models seem to approximate measured power losses relatively well. The Steinmetz law is slightly more consistent with experimental data. For steels (Figs. 3 and 4), the situation is more diversified. The Rayleigh model provides a significantly worse approximation, especially for points near the end of the measurement range. However, as it was previously presented in [25], the transition from the lenticular loop to the sigmoidal loop of investigated steels is much more rapid than in the case of ferrites and takes place in the fields much below the coercive field of the material. This results in a less accurate approximation of magnetic parameters, including

TABLE III

Statistical metrics of Rayleigh model and Steinmetz law for investigated materials: $Ni_{0.36}Zn_{0.64}Fe_2O_4$ (A), $Ni_{0.36}Zn_{0.67}Fe_{1.97}O_4$ (B), X30Cr13 (C), and 13CrMo4-5 (D).

Material	Rayleigh model		Steinmetz law	
	R^2 [–]	NRMSD [%]	R^2 [–]	NRMSD [%]
A	0.972	5.48	0.995	2.34
B	0.972	5.45	0.995	2.30
C	0.876	11.97	0.998	1.50
D	0.918	9.66	0.997	1.99

power loss, for the fields near the Rayleigh region limit. On the other hand, the Steinmetz law was proven to be valid also for the fields beyond the Rayleigh region, so the decrease in approximation quality near the region limit does not occur.

The quality of approximation for both models was evaluated with two statistical metrics. The determination coefficient R^2 was calculated according to the following formula [26]

$$R^2 = 1 - \frac{\sum_{i=1}^{n}\left(P_{Hi}-\hat{P}_{Hi}\right)^2}{\sum_{i=1}^{n}\left(P_{Hi}-\frac{1}{n}\sum_{i=1}^{n}P_{Hi}\right)^2}, \tag{15}$$

where P_{Hi} is the experimental value, $\hat{P}_{Hi}$ — value estimated by the model, and n — number of measurement points. Root-mean-square deviation (RMSD) normalized by the range of measured values — NRMSD — is expressed as [26]

$$\text{NRMSD} = \frac{1}{\Delta P_{Hi}}\sqrt{\frac{1}{n}\sum_{i=1}^{n}\left(P_{Hi}-\hat{P}_{Hi}\right)^2}, \tag{16}$$

where ΔP_{Hi} is the range of measured values of P_{Hi}. The metrics characterizing both models were calculated for each investigated material. The resulting values are summarized in Table III.

The presented results indicate that for all investigated materials, the Steinmetz law provides better approximation in terms of both R^2 and NRMSD. Again, the difference is especially significant for steels. Values of NRMSD for Steinmetz law are in this case five to eight times lower than for the Rayleigh model. However, both models allow us to relatively well estimate the power loss P_H with R^2 over 0.9 (except for the Rayleigh model for X30Cr13 steel). The advantage of Steinmetz law results partially from the direct fitting of the model curve to the experimental data, while coefficients of the Rayleigh model are determined on the basis of fitting the Rayleigh law of magnetization (1) to the commutation curve. Such indirect determination of model coefficients might negatively influence the quality of approximation.

5. Conclusions

The experimental data presented in the paper allowed us to compare the power loss approximation capability in low magnetizing fields of two simple mathematical models: the Rayleigh model of hysteresis and Steinmetz law. Both models were applied to the set of experimental data obtained for two different kinds of soft magnetic materials: ferrimagnetic Ni–Zn ferrites and ferromagnetic structural steels.

The modeling results indicate that both models approximate the power loss in the Rayleigh region with satisfying quality. For ferrites, the determination coefficient R^2 is relatively high, slightly preferring Steinmetz law. In the case of steels, the difference in the quality of description is more prominent, and the statistical metrics of the Rayleigh model are significantly worse than those of Steinmetz law. The reason is probably a more rapid transformation of the hysteresis loop shape with increasing field amplitude, which does not follow the Rayleigh description well, but is in good agreement with the Steinmetz equation developed for a wider range of magnetizing fields, including high permeability region.

Despite the fact that both investigated models can be considered satisfyingly accurate in the estimation of power losses of soft magnetic materials in low magnetizing fields, further investigation is still required to validate the models for a higher range of magnetizing field frequency. Also, the investigation of modified versions of Steinmetz law seems to be interesting and may lead to further improvement of the approximation quality.

References

[1] R. Hasegawa, D. Azuma, *J. Magn. Magn. Mater.* **320**, 2451 (2008).

[2] F. Liorzou, B. Phelps, D.L. Atherton, *IEEE Trans. Magn.* **36**, 418 (2000).

[3] R.H. Pry, C.P. Bean, *J. Appl. Phys.* **29**, 532 (1958).

[4] T. Matsuo, M. Shimasaki, *IEEE Trans. Magn.* **42**, 919 (2006).

[5] K. Chwastek, A.P.S. Baghel, P. Borowik, B.S. Ram, S.V. Kulkarni, in: *2016 Progress in Applied Electrical Engineering (PAEE), Koscielisko-Zakopane*, IEEE, 2026.

[6] G. Bertotti, *IEEE Trans. Magn.* **24**, 621 (1988).

[7] G. Bertotti, *Hysteresis in Magnetism for Physicists, Materials Scientists, and Engineers*, Acad. Press, San Diego 1998.

[8] B. Koprivica, K. Chwastek, *Acta Phys. Pol. A* **136**, 709 (2019).

[9] J. Szczygłowski, P. Kopciuszewski, K. Chwastek, M. Najgebauer, W. Wilczyński, *Arch. Electr. Eng.* **60**, 59 (2011).

[10] B.D. Cullity, C.D. Graham, *Introduction to Magnetic Materials*, John Wiley & Sons, New York 2009.

[11] W.B. Ellwood, *Physics* **6**, 215 (1935).

[12] Yu.N. Starodubtsev, V.A. Kataev, K.O. Bessonova, V.S. Tsepelev, *J. Magn. Magn. Mater.* **479**, 19 (2019).

[13] D.C. Jiles, *Introduction to Magnetism and Magnetic Materials*, Chapman & Hall, London 1998.

[14] Yu.F. Ponomarev, *Phys. Met. Metallogr.* **104**, 469 (2007).

[15] J. Kováč, B. Kunca, L. Novák, *J. Magn. Magn. Mater.* **502**, 166555 (2020).

[16] Lord Rayleigh, *Philos. Mag.* **23**, 225 (1887).

[17] C.P. Steinmetz, *Trans. AIEE* **IX**, 1 (1892).

[18] F.J.G. Landgraf, M. Emura, M.F. de Campos, *J. Magn. Magn. Mater.* **320**, e531 (2008).

[19] D. Gzieł, M. Najgebauer, *Przegląd Elektrotechniczny* **97**, 238 (2020).

[20] M. Najgebauer, *Acta Phys. Pol. A* **131**, 1225 (2017).

[21] M. Najgebauer, in: *2019 Progress in Applied Electrical Engineering (PAEE), Koscielisko-Zakopane*, IEEE, 2019.

[22] M. Kachniarz, R. Szewczyk, *J. Electr. Eng.* **66**, 82 (2015).

[23] M. Kachniarz, K. Kołakowska J. Salach, R. Szewczyk, P. Nowak *Acta Phys. Pol. A* **133**, 660 (2018).

[24] P. Jabłoński, M. Najgebauer, M. Bereźnicki, *Energies* **15**, 2869 (2022).

[25] M. Kachniarz, R. Szewczyk, *Acta Phys. Pol. A* **131**, 1244 (2017).

[26] G. James, D. Witten, T. Hastie, R. Tibshirani, *An Introduction to Statistical Learning*, Springer, New York 2013.